

ORDERED MESOPOROUS CARBONS AND ITS
ALGINATE COMPOSITE ADSORBENTS:
SYNTHESES, CHARACTERIZATIONS AND
ADSORPTION PERFORMANCES FOR
METHYLENE BLUE, CHLORAMPHENICOL AND
RIBOFLAVIN

AZAM TAUFIK BIN MOHD DIN

UNIVERSITI SAINS MALAYSIA
2014

**ORDERED MESOPOROUS CARBONS AND ITS ALGINATE COMPOSITE
ADSORBENTS: SYNTHESSES, CHARACTERIZATIONS AND ADSORPTION
PERFORMANCES FOR METHYLENE BLUE, CHLORAMPHENICOL AND
RIBOFLAVIN**

by

AZAM TAUFIK BIN MOHD DIN

**Thesis submitted in fulfillment of the
requirements for the degree of
Doctor of Philosophy**

AUGUST 2014

ACKNOWLEDGEMENTS

First and foremost, praises to the Almighty God, Allah S.W.T. upon the completion of this thesis. A special thanks to Prof. Dr. Bassim H. Hameed for his wonderful supervision and guidance. Thanks also to Assoc. Prof. Dr. Mohd Azmier bin Ahmad for his valuable comments and encouragement.

My sincere gratitude to the Dean of School of Chemical Engineering (SCE), Prof. Dr. Azlina binti Harun @ Kamarudin and the former Dean, Prof. Dr. Abdul Latif bin Ahmad for the administration support related to my PhD study. Also, Assoc. Prof. Dr. Mohamad Zailani bin Abu Bakar for the encouragement and endless assistances. My special thanks to all SCE academic, administration and technical staff. Mr. Muhammad Ismail bin Abu Talib, Mr. Mohd Roqib bin Mohd Rashidi and Mr. Shamsul Hidayat bin Shaharan, thanks for the prompt supports. My sincere gratitude to Mr. Masrul Mansor from School of Biological sciences, USM and Mr. Yushamdan bin Yusof from School of Physics, USM.

Special note to my mother, Mrs. Wan Sapiah binti Wan Sulaiman - I'm grateful for your love and endless prayers. Dr. Sharifah Azdiana binti Tuan Din, thanks for being a lovely wife. Little Malika Irdina binti Azam Taufik, truly you are my heart and my soul. My brothers and sisters, thanks for the motivation. To my dear friends, thanks for your kind supports and soothing words.

Finally, for those who have directly and indirectly helped me in this project, thank you very much.

TABLE OF CONTENTS

	Page
ACKNOWLEDGEMENTS	ii
TABLE OF CONTENTS	iii
LIST OF TABLES	xi
LIST OF FIGURES	xv
LIST OF PLATES	xx
LIST OF SYMBOLS	xxi
LIST OF ABBREVIATIONS	xxiv
ABSTRAK	xxv
ABSTRACT	xxvii
CHAPTER ONE: INTRODUCTION	
1.1 Ordered mesoporous carbons	1
1.2 Alginate composite adsorbents	4
1.3 Dyes and pharmaceutical compounds	5
1.4 Adsorption process	8
1.5 Problem statements	8
1.6 Research objectives	11
1.7 Scope of research	12
1.8 Organization of the thesis	13

CHAPTER TWO: LITERATURE REVIEW

2.0	Ordered mesoporous materials	15
2.1	Ordered mesoporous carbons	17
2.2	Synthesis of ordered mesoporous carbons	19
	2.2.1 Nanocasting	20
	2.2.2 Soft-templating	25
2.3	Physical and chemical properties of ordered mesoporous carbons	26
	2.3.1 Yields	26
	2.3.2 Surface area and pore volume	26
	2.3.3 Pore size distribution	29
	2.3.4 Surface morphology	31
	2.3.5 X-ray diffraction analysis	31
	2.3.6 Surface chemistry	33
2.4	Alginate-ordered mesoporous carbon composite beads	35
2.5	Adsorption	36
	2.5.1 Adsorption of methylene blue	37
	2.5.2 Adsorption of chloramphenicol	37
	2.5.3 Adsorption of riboflavin	41
2.6	Batch adsorption studies	43
	2.6.1 Batch process variables	43
2.7	Adsorption isotherms	45
	2.7.1 Two-parameter adsorption isotherms	48
	2.7.2 Three-parameter adsorption isotherms	51
2.8	Thermodynamics	53

2.9	Adsorption kinetics	54
	2.9.1 The pseudo-first order kinetic model	54
	2.9.2 The pseudo-second order kinetic model	55
2.9.3	Elovich kinetic model	56
2.10	Column adsorption operation	57
	2.10.1 Process variables	58
2.11	Dynamic adsorption models	62
	2.11.1 Thomas model	62
	2.11.2 Modified Dose-Response model	63
	2.11.3 Bed Depth Service Time model	64
2.12	Adsorbent reusability	65
2.13	Summary	70

CHAPTER THREE: MATERIALS AND METHODS

3.1	Materials and chemicals	71
3.2	Model adsorbates	71
3.3	Characterization of materials	75
	3.3.1 Surface area analysis	75
	3.3.2 Elemental analysis	75
	3.3.3 Proximate analysis	76
	3.3.4 Surface morphology	76
	3.3.5 Energy dispersive x-ray analysis (EDX)	77
	3.3.6 Textural analysis	77
	3.3.7 X-ray diffraction analysis (XRD)	77
	3.3.8 Surface chemistry	77

3.3.9	Determination of pH_{ZPC}	78
3.4	Synthesis of materials	78
3.4.1	Preparation of hexagonal mesoporous silica	78
3.4.2	Nanocasting of ordered mesoporous carbon	79
3.4.2 (a)	Effect of carbonization temperatures	81
3.4.2 (b)	Effect of dwelling time	81
3.4.2 (c)	Effect of heating rates	81
3.4.2 (d)	Effect of polyethylene glycol 400 loading	82
3.4.3	Modification of OMC	83
3.4.4	Preparation of alginate bead adsorbents	83
3.5	Experimental procedures	83
3.5.1	Batch adsorption studies	83
3.5.1 (a)	Effect of initial concentrations	84
3.5.1 (b)	Effect of temperatures	84
3.5.1 (c)	Effect of pH	84
3.5.2	Continuous adsorption studies	85
3.5.2 (a)	Effect of flow rate	85
3.5.2 (b)	Effect of initial concentration	85
3.5.2 (c)	Effect of bed height	85
3.5.3	In-situ column regeneration studies	86
3.6	Concentration analysis	87
3.7	Non-linear error analyses	89
3.8	Safety and environmental precautions.	90

CHAPTER FOUR: RESULTS AND DISCUSSION

4.1	Nanocasting of ordered mesoporous carbons	91
4.1.1	Effect of carbonization temperature	92
4.1.2	Effect of dwelling time	94
4.1.3	Effect of heating rate	96
4.1.4	Effect of polyethylene glycol 400 loading	99
4.1.5	Modification of ordered mesoporous carbons	101
4.2	Characteristics of hexagonal mesoporous silica, ordered mesoporous carbons and its alginate composite adsorbents	102
4.2.1	Surface area properties	102
4.2.2	Scanning electron microscopy (SEM)	106
4.2.3	Transmission electron microscopy (TEM)	109
4.2.4	X-ray diffraction analysis (XRD)	113
4.2.5	Energy dispersive X-ray (EDX)	115
4.2.6	Elemental analysis (EA)	116
4.2.7	Surface chemistry	118
4.3	Batch adsorption studies	120
4.3.1	Effect of initial concentrations	120
4.3.2	Effect of nature of solutes	125
4.3.3	Effect of pH	128
4.3.4	Effect of temperatures	132
4.3.4 (a)	Methylene blue	132
4.3.4 (b)	Chloramphenicol	134
4.3.4 (a)	Riboflavin	134
4.3.5	Adsorption isotherms	137

4.3.5 (a)	Two-parameter adsorption isotherm models	137
4.3.5 (b)	Three-parameter adsorption isotherm models	152
4.3.6	Adsorption kinetics	164
4.3.6 (a)	Methylene blue	164
4.3.6 (b)	Chloramphenicol	168
4.3.6 (a)	Riboflavin	173
4.3.7	Thermodynamics	177
4.3.8	Adsorption mechanism and batch adsorption performance comparison	180
4.3.8 (a)	Methylene blue	180
4.3.8 (b)	Chloramphenicol	182
4.3.8 (a)	Riboflavin	184
4.4	Column adsorption studies	184
4.4.1	Effect of flow rates	186
4.4.1 (a)	Non-modified alginate-ordered mesoporous carbon composite beads	186
4.4.1 (b)	Modified alginate-ordered mesoporous carbon composite beads	188
4.4.2	Effect of initial concentrations	190
4.4.2 (a)	Non-modified alginate-ordered mesoporous carbon composite beads	190
4.4.2 (b)	Modified alginate-ordered mesoporous carbon composite beads	192
4.4.3	Effect of bed heights	194

4.4.3 (a)	Non-modified alginate-ordered mesoporous carbon composite beads	194
4.4.3 (b)	Modified alginate-ordered mesoporous carbon composite beads	196
4.4.4	Breakthrough characteristics and dynamics	199
4.4.4 (a)	Thomas model	199
4.4.4 (b)	Modified Dose-Response model	202
4.4.4 (c)	Bed Depth Service Time model	209
4.5	In-situ column regeneration studies	213

CHAPTER FIVE: CONCLUSIONS AND RECOMMENDATIONS

5.1	Conclusions	218
5.2	Recommendations	219

REFERENCES

APPENDIXES

Appendix A	Concentration analysis calibration curves	249
Appendix B	EDX spectra	250
Appendix C	Adsorption profiles of MB, CPC and RB on ABA-16 at 313 and 323 K	252
Appendix D	Adsorption profiles of MB, CPC and RB on MABA-16 at 313 and 323 K	254
Appendix E	Fittings of two-parameter adsorption isotherm models on ABA-16	256

Appendix F	Fittings of two-parameter adsorption isotherm models on MABA-16	258
Appendix G	Fittings of three-parameter adsorption isotherm models on ABA-16	260
Appendix H	Fittings of three-parameter adsorption isotherm models on MABA-16	262
Appendix I	Kinetic model constants and non-linear errors for MB adsorption on ABA-16 and MABA-16	264
Appendix J	Kinetic model constants and non-linear errors for CPC adsorption on ABA-16 and MABA-16	266
Appendix K	Kinetic model constants and non-linear errors for RB adsorption on ABA-16 and MABA-16	268
Appendix L	Thomas model plots on AG/ABA-16 composite beads	270
Appendix M	Thomas model plots on AG/MABA-16 composite beads	272
Appendix N	MDR model plots on AG/ABA-16 and AG/MABA-16 composite beads	274
LIST OF PUBLICATIONS		278

LIST OF TABLES

Table 2.1	Various carbonization conditions applied for OMCs syntheses	24
Table 2.2	Surface area and pore volume properties of OMCs	30
Table 2.3	Methylene blue adsorption capacity on various sorbent media	38
Table 2.4	Antibiotics adsorption capacity on various sorbent media	40
Table 2.5	Vitamins adsorption capacity on various sorbent media	42
Table 2.6	Batch adsorption process conditions for various adsorption systems	46
Table 2.7	Column adsorption process conditions for various adsorption systems	60
Table 2.8	Comparison of various type of regeneration methods (Cavalcante Jr, 2000)	67
Table 2.9	Summary of regeneration methods for liquid-phase adsorption systems	68
Table 3.1	List of chemicals and materials used in this research	73
Table 3.2	General information of MB, CPC and RB	74
Table 3.3	Operating conditions for nanocasting of ordered mesoporous carbons	82
Table 4.1	Carbon yields and MB removal performances on the prepared ordered mesoporous carbons at various parameters	92
Table 4.2	Surface area properties of ordered mesoporous carbons prepared at different carbonization temperatures	94
Table 4.3	Surface area properties of ordered mesoporous carbons prepared at different dwelling time	96
Table 4.4	Surface area properties of ordered mesoporous carbons prepared at different heating rate	98
Table 4.5	Surface area properties of ordered mesoporous carbons prepared at various PEG-400 loading	100

Table 4.6	Surface area properties of the selected adsorbents	103
Table 4.7	Summary of EDX results	115
Table 4.8	Elemental and proximate analysis of the selected adsorbents	117
Table 4.9	Langmuir, Freundlich, Tempkin and D-R constants of MB/ABA-16 adsorption system	138
Table 4.10	Langmuir, Freundlich, Tempkin and D-R constants for MB/MABA-16 adsorption system	142
Table 4.11	Langmuir, Freundlich, Tempkin and D-R constants for CPC/ABA-16 adsorption system	144
Table 4.12	Langmuir, Freundlich, Tempkin and D-R constants for CPC/MABA-16 adsorption system	147
Table 4.13	Langmuir, Freundlich, Tempkin and D-R constants for RB/ABA-16 adsorption system	149
Table 4.14	Langmuir, Freundlich, Tempkin and D-R constants for RB/MABA-16 adsorption system	151
Table 4.15	Koble-Corrigan, Redlich-Peterson, Sips and Toth constants for MB/ABA-16 adsorption system	153
Table 4.16	Koble-Corrigan, Redlich-Peterson, Sips and Toth constants for MB/MABA-16 adsorption system	155
Table 4.17	Koble-Corrigan, Redlich-Peterson, Sips and Toth constants for CPC/ABA-16 adsorption system	157
Table 4.18	Koble-Corrigan, Redlich-Peterson, Sips and Toth constants for CPC/MABA-16 adsorption system	159
Table 4.19	Koble-Corrigan, Redlich-Peterson, Sips and Toth constants for RB/ ABA-16 adsorption system	161
Table 4.20	Koble-Corrigan, Redlich-Peterson, Sips and Toth constants for RB/MABA-16 adsorption system	163
Table 4.21	Summary of kinetic models constants and its non-linear errors for MB/ABA-16 adsorption system at 303 K	167
Table 4.22	Summary of kinetic models constants and its non-linear errors for MB/ MABA-16 adsorption system at 303 K	167
Table 4.23	Summary of kinetic models constants and its non-linear errors for CPC/ ABA-16 adsorption system at 303 K	172
Table 4.24	Summary of kinetic models constants and its non-linear errors for CPC/MABA-16 adsorption system at 303 K	172

Table 4.25	Summary of kinetic models constants and its non-linear errors for RB/ABA-16 adsorption system at 303 K	176
Table 4.26	Summary of kinetic models constants and its non-linear errors for RB/MABA-16 adsorption system at 303 K	176
Table 4.27	Thermodynamics properties of the selected adsorption systems at 303, 313 and 323 K	178
Table 4.28	Comparative MB adsorption capacity on various materials	181
Table 4.29	Comparative CPC adsorption capacity on various materials	183
Table 4.30	Comparative RB adsorption capacity on various materials	185
Table 4.31	The column adsorption performances of MB, CPC and RB on AG/ABA-16 at different flow rates ($C_0 = 50 \text{ mg.L}^{-1}$, $BH = 2 \text{ cm}$ and $T = 303 \text{ K}$)	188
Table 4.32	Column adsorption performances of MB, CPC and RB on AG/MABA-16 at different flow rates ($C_0 = 50 \text{ mg.L}^{-1}$, $BH = 2 \text{ cm}$ and $T = 303 \text{ K}$)	190
Table 4.33	The column adsorption performances of MB, CPC and RB on AG/ABA-16 at different initial concentrations ($F = 10 \text{ mL.min}^{-1}$, $BH = 2 \text{ cm}$ and $T = 303 \text{ K}$)	192
Table 4.34	The column adsorption performances of MB, CPC and RB on AG/MABA-16 at different initial concentrations ($F = 10 \text{ mL.min}^{-1}$, $BH = 2 \text{ cm}$ and $T = 303 \text{ K}$)	194
Table 4.35	The column adsorption performances of MB, CPC and RB on AG/ABA-16 at different bed heights ($F = 10 \text{ mL.min}^{-1}$, $C_0 = 50 \text{ mg.L}^{-1}$ and $T = 303 \text{ K}$)	197
Table 4.36	The column adsorption performances of MB, CPC and RB on MABA-16 at different bed heights ($F = 10 \text{ mL.min}^{-1}$, $C_0 = 50 \text{ mg.L}^{-1}$ and $T = 303 \text{ K}$)	197
Table 4.37	Thomas model constants and its non-linear errors AG/ABA-16 composite beads	200
Table 4.38	Thomas model constants and its non-linear errors of AG/MABA-16 composite beads	203
Table 4.39	Modified Dose-Response model constants and its non-linear errors of AG/ABA-16 composite beads	205
Table 4.40	Modified Dose-Response model constants and its non-linear errors of AG/MABA-16 composite beads	207

Table 4.41	BDST model constants and its non-linear errors AG/ABA-16 composite beads	211
Table 4.42	Bed Depth Service Time model constants and its non-linear errors of AG/MABA-16 composite beads	211
Table 4.43	Experimental and BDST model predicted breakthrough time at $C/C_0 = 0.5$	214
Table 4.44	Regeneration performance of AG/ABA-16 and AG/MABA-16 composite beads on MB, CPC and RB	217

LIST OF FIGURES

Figure 1.1	The progress in articles publications (ISI-cited) related to ordered mesoporous carbon (key word: ordered mesoporous carbon, date of search: 15 February 2014)	3
Figure 1.2	Pharmaceutical waste detected in sewage treatment plant near Langat River, Selangor (Al-Odaini et al., 2013)	6
Figure 2.1	Synthesis route for highly ordered mesoporous carbon (Guo et al., 2013)	21
Figure 2.2	Nitrogen adsorption isotherms (Smith, 1981)	28
Figure 2.3	Classification of adsorption/desorption hysteresis loops (Kruk and Jaroniec, 2001)	28
Figure 2.4	Various types of pore topologies of ordered mesoporous materials; from left: 2-D hexagonal (p6mm), 3-D cubic (Ia 3 d), 3-D body-centered cubic (Im 3 m) and 3-D face-centered cubic (Fm 3 m) (Klabunde and Richards, 2001)	32
Figure 2.5	Common acidic functional group available in activated carbon (Yang, 2005)	34
Figure 2.6	Common basic functional group available in activated carbon (Yang, 2005)	34
Figure 2.7	Typical breakthrough profiles in column operation (Barros et al., 2013)	58
Figure 3.1	Research flow diagram	72
Figure 3.2	Molecular structures of (a) MB, (b) CPC and (c) RB (Sigma-Aldrich, 2014)	74
Figure 3.3	Schematic drawing of vertical cylindrical reactor furnace	80
Figure 3.4	Column adsorption system set up	86
Figure 4.1	Effect of carbonization temperature on the carbon yields and MB removal	93
Figure 4.2	Effect of dwelling time on the carbon yields and MB removal	95
Figure 4.3	Effect of heating rate on the carbon yields and MB removal	98

Figure 4.4	Effect of polyethylene glycol 400 loading on the carbon yields and MB removal	99
Figure 4.5	MB removal profiles over acetic acid concentration variations at 303 K	102
Figure 4.6	Nitrogen adsorption/desorption isotherms at 77 K	104
Figure 4.7	Barrett-Joyner-Haleda pore size distributions	105
Figure 4.8	Harkin-Jura t-plots	106
Figure 4.9	XRD patterns of HMS, ABA-16 and MABA-16	114
Figure 4.10	A proposed hexagonal structure of HMS, ABA-16 and FABA-16	115
Figure 4.11	FTIR spectra of silica, carbon, alginate and its composite materials	119
Figure 4.12	Adsorption profiles of (a) MB, (b) CPC and (c) RB at 303 K on ABA-16 for different initial concentrations	121
Figure 4.13	Adsorption profiles of (a) MB, (b) CPC and (c) RB at 303 K on MABA-16 for different initial concentrations	124
Figure 4.14	Adsorption isotherms of MB, CPC and RB on non-modified ordered mesoporous carbon, ABA-16 at (a) 303 K, (b) 313 K and (c) 323 K	126
Figure 4.15	Adsorption isotherms of MB, CPC and RB on modified ordered mesoporous carbon, MABA-16 at (a) 303 K, (b) 313 K and (c) 323 K	129
Figure 4.16	Adsorption equilibrium uptakes of (a) MB, (b) CPC and (c) RB on ABA-16 and MABA-16 at 303 K	131
Figure 4.17	Adsorption isotherms of MB on (a) ABA-16 and (b) MABA-16 at 303, 313 and 323 K	133
Figure 4.18	Adsorption isotherms of CPC on (a) ABA-16 and (b) MABA-16 at 303, 313 and 323 K	135
Figure 4.19	Adsorption isotherms of RB on (a) ABA-16 and (b) MABA-16 at 303, 313 and 323 K	136
Figure 4.20	Fittings of the selected two-parameter adsorption isotherm models on MB/ABA-16 adsorption system at 303 K	140

Figure 4.21	Fittings of the selected two-parameter adsorption isotherm models on MB adsorption onto MABA-16 at 303 K	143
Figure 4.22	Fittings of the selected two-parameter adsorption isotherm models on CPC adsorption onto ABA-16 at 303 K	145
Figure 4.23	Fittings of the selected two-parameter adsorption isotherm models on CPC adsorption onto MABA-16 at 303 K	146
Figure 4.24	Fittings of the selected two-parameter adsorption isotherm models on RB adsorption onto ABA-16 at 303 K	150
Figure 4.25	Fittings of the selected two-parameter adsorption isotherm models on RB adsorption onto MABA-16 at 303 K	152
Figure 4.26	Fittings of the selected three-parameter adsorption isotherm models on MB adsorption onto ABA-16 at 303 K	154
Figure 4.27	Fittings of the selected three-parameter adsorption isotherm models on MB adsorption onto MABA-16 at 303 K	154
Figure 4.28	Fittings of the selected three-parameter adsorption isotherm models on CPC adsorption onto ABA-16 at 303 K	156
Figure 4.29	Fittings of the selected three-parameter adsorption isotherm models on CPC adsorption onto MABA-16 at 303 K	158
Figure 4.30	Fittings of the selected three-parameter adsorption isotherm models on RB adsorption onto ABA-16 at 303 K	160
Figure 4.31	Fittings of the selected three-parameter adsorption isotherm models on RB adsorption onto MABA-16 at 303 K	162
Figure 4.32	Non-linear fittings of (a) Pseudo-first order, (b) Pseudo-second order and (c) Elovich kinetic models on MB/ABA-16 at 303 K	165
Figure 4.33	Non-linear fittings of (a) Pseudo-first order, (b) Pseudo-second order and (c) Elovich kinetic models on MB/MABA-16 at 303 K	166
Figure 4.34	Non-linear fittings of (a) Pseudo-first order, (b) Pseudo-second order and (c) Elovich kinetic models on CPC/ABA-16 at 303 K	170
Figure 4.35	Non-linear fittings of (a) Pseudo-first order, (b) Pseudo-second order and (c) Elovich kinetic models on CPC/MABA-16 at 303 K	171

Figure 4.36	Non-linear fittings of (a) Pseudo-first order, (b) Pseudo-second order and (c) Elovich kinetic models on RB/ABA-16 at 303 K	174
Figure 4.37	Non-linear fittings of (a) Pseudo-first order, (b) Pseudo-second order and (c) Elovich kinetic models on RB/MABA-16 at 303 K	175
Figure 4.38	FTIR spectra of fresh and after MB adsorption ordered mesoporous carbons	181
Figure 4.39	FTIR spectra of fresh and after CPC adsorption ordered mesoporous carbons	183
Figure 4.40	FTIR spectra of fresh and after RB adsorption ordered mesoporous carbons	185
Figure 4.41	Adsorption breakthrough curves of (a) MB, (b) CPC and (c) RB on AG/ABA-16 composite beads at different flow rates ($C_0 = 50 \text{ mg.L}^{-1}$, $BH = 2 \text{ cm}$ and $T = 303 \text{ K}$)	187
Figure 4.42	Adsorption breakthrough curves of (a) MB, (b) CPC and (c) RB on AG/MABA-16 composite beads at different flow rates ($C_0 = 50 \text{ mg.L}^{-1}$, $BH = 2 \text{ cm}$ and $T = 303 \text{ K}$)	189
Figure 4.43	Adsorption breakthrough curves of (a) MB, (b) CPC and (c) RB on AG/ABA-16 composite beads at different initial concentrations ($F = 10 \text{ mL.min}^{-1}$, $BH = 2 \text{ cm}$ and $T = 303 \text{ K}$)	191
Figure 4.44	Adsorption breakthrough curves of (a) MB, (b) CPC and (c) RB on AG/MABA-16 composite beads at different initial concentrations ($F = 10 \text{ mL.min}^{-1}$, $BH = 2 \text{ cm}$ and $T = 303 \text{ K}$)	193
Figure 4.45	Adsorption breakthrough curves of (a) MB, (b) CPC and (c) RB on AG/ABA-16 composite beads at different bed heights ($F = 10 \text{ mL.min}^{-1}$, $C_0 = 50 \text{ mg.L}^{-1}$ and $T = 303 \text{ K}$)	195
Figure 4.46	Adsorption breakthrough curves of (a) MB, (b) CPC and (c) RB on AG/MABA-16 composite beads at different bed heights ($F = 10 \text{ mL.min}^{-1}$, $C_0 = 50 \text{ mg.L}^{-1}$ and $T = 303 \text{ K}$)	198
Figure 4.47	Experimental and predicted Thomas model adsorption breakthrough dynamics of (a) MB, (b) CPC and (c) RB on AG/ABA-16 at different flow rates ($C_0 = 50 \text{ mg.L}^{-1}$, $BH = 2 \text{ cm}$ and $T = 303 \text{ K}$)	201
Figure 4.48	Experimental and predicted Thomas model adsorption breakthrough dynamics of (a) MB, (b) CPC and (c) RB on AG/MABA-16 at different flow rates ($C_0 = 50 \text{ mg.L}^{-1}$, $BH = 2 \text{ cm}$ and $T = 303 \text{ K}$)	204

Figure 4.49	Experimental and predicted MDR model adsorption breakthrough dynamics of (a) MB, (b) CPC and (c) RB on AG/ABA-16 at different flow rates ($C_0 = 50 \text{ mg.L}^{-1}$, BH = 2 cm and T = 303 K)	206
Figure 4.50	Experimental and predicted MDR model adsorption breakthrough dynamics of (a) MB, (b) CPC and (c) RB on AG/MABA-16 at different flow rates ($C_0 = 50 \text{ mg.L}^{-1}$, BH = 2 cm and T = 303 K)	208
Figure 4.51	Bed Depth Time Service model for (a) MB, (b) CPC and (c) RB on AG/ABA-16 composite beads at different bed heights ($C_0 = 50 \text{ mg.L}^{-1}$, F = 10 ml/min and T = 303 K)	210
Figure 4.52	Bed Depth Time Service model for (a) MB, (b) CPC and (c) RB on AG/MABA-16 composite beads at different bed heights ($C_0 = 50 \text{ mg.L}^{-1}$, F = 10 ml/min and T = 303 K)	212
Figure 4.53	Breakthrough performances of MB adsorption on regenerated AG/MABA-16 composite beads	216
Figure 4.54	Breakthrough performances of CPC adsorption on regenerated AG/ABA-16 composite beads	216
Figure 4.55	Breakthrough performances of RB adsorption on regenerated AG/ABA-16 composite beads	216

LIST OF PLATES

Plate 1.1	TEM images of (A) SBA-15 (template) (B) CMK-3 (carbon replica), (C) KIT-6 (template) and (D) CMK-8 (carbon replica). (Goscianska et al. 2013)	2
Plate 2.1	SEM image of activated carbon produced from banana frond (Foo et al., 2013)	18
Plate 2.2	TEM of ordered mesoporous carbon derived from phenol/formaldehyde as a carbon source (Cai et al., 2013)	18
Plate 2.3	Surface morphology of OMCs obtained from SEM (above) and intrinsic pore structures inspected by TEM (below) (Kubo et al., 2011)	32
Plate 4.1	Surface morphology of hexagonal mesoporous silica at (a) 1000x, (b) 2500x and (c) 5000x magnifications.	107
Plate 4.2	Surface morphology of non functionalized ordered mesoporous carbon, ABA-16 at (a) 1000x, (b) 2500x and (c) 10000x magnifications.	107
Plate 4.3	Surface morphology of functionalized ordered mesoporous carbon, FABA-16 at (a) 2500x and (b) 5000x magnifications.	108
Plate 4.4	Surface morphology of (a) AG bead at 500x magnification, (b) AG/ABA-16 at 1000x magnification and (c) AG/FABA-16 at 1000x magnification.	108
Plate 4.5	Cross-sectional view of HMS internal structure at different spots (a) and (b) and its perpendicular views at (c) and (d) spots. (Magnifications 45000x)	110
Plate 4.6	Cross-sectional view of non-functionalized ordered mesoporous carbon, ABA-16 internal structure at different spots (a) and (b) and its perpendicular views at (c) and (d) spots. (Magnifications 20000x)	111
Plate 4.7	Cross-sectional view of functionalized ordered mesoporous carbon, FABA-16 internal structure at different spots (a) and (b) and its perpendicular views at (c) and (d) spots. (Magnifications 20000x)	112

LIST OF SYMBOLS

A	R-P model constant	$(L.g^{-1})$
a_{KC}	K-C model constant	$(mg.g^{-1})(L.mg^{-1})$
a_L	Langmuir isotherm constant	$L.mg^{-1}$
B	R-P model constant	$(L(mg^{-1-(1/A)})^{-1})$
b_{KC}	K-C model constant	$(L.mg^{-1})$
B_D	D-R model constant	$mol^2.kJ^{-2}$
B_T	Heat of adsorption	$J.mol^{-1}$
b_T	Tempkin constant	Dimensionless
B_{TO}	Toth model constant	$(m^3.g^{-1})$
C_b	breakthrough dye concentration	$(mg.L^{-1})$
C_e	Equilibrium concentration of liquid phase	$mg.L^{-1}$
C_0	Initial concentration of liquid phase	$mg.L^{-1}$
C_t	Concentration of liquid phase at time, t	$mg.L^{-1}$
E	Free mean energy	$kJ.mol^{-1}$
g	R-P model constant	Dimensionless
H	Bed height	cm
K_1	Rate constant of pseudo-first order sorption	min^{-1}
K_2	Rate constant of pseudo-second order sorption	$g.(mg.min)^{-1}$
K_L	Langmuir isotherm constant	$L.g^{-1}$
K_F	Freundlich constant	$(mg.g^{-1})(L.mg^{-1})^{1/n}$
K_T	Equilibrium binding constant	$L.g^{-1}$
K_{TO}	Toth model constant	$(mg.g^{-1})(m^3.g^{-1})$
K_s	Sips model constant	$(L.g^{-1})$

m	Mass of material	g
N	Number of data points	Dimensionless
n	Freundlich heterogeneity factor	Dimensionless
n	K-C model constant	Dimensionless
N_0	sorption capacity of bed	mg.L ⁻¹
n_{TO}	Toth model constant	Dimensionless
P/P_0	Relative pressure	Dimensionless
Q	Volumetric flow rate	mL.min ⁻¹
Q_0	Langmuir constant related to maximum surface coverage of adsorbent	mg.g ⁻¹
q_D	D-R model constant	mg.g ⁻¹
q_e	Amount of solute adsorb per unit weight of adsorbent at equilibrium	mg.g ⁻¹
$q_{e,calc}$	Equilibrium concentration obtained from the model	mg.g ⁻¹
$q_{e,exp}$	Equilibrium concentration obtained from the experiment	mg.g ⁻¹
q_s	Sips model constant	(mg.g ⁻¹)
q_t	Amount of solute adsorb per unit weight of adsorbent at time, t	mg.g ⁻¹
R_L	Langmuir separation factor	Dimensionless
r^2	Coefficient of determination	Dimensionless
t	Contact time	min
t_{total}	Total flow time	min
U	linear velocity	(cm.min ⁻¹)
V	Volume of solution	L
Z	Bed height of the column	cm
α	Sips model constant	Dimensionless

α	Elovich initial rate	(mg.(g.min ⁻¹))
β	Elovich model constant	g.mg ⁻¹

LIST OF ABBREVIATIONS

ARE	Average relative error
BDST	Bed Depth Service Time model
BET	Brunauer–Emmett–Teller
BJH	Barrett-Joyner-Halenda
CPC	Chloramphenicol
D-R	Dubinin-Radushkevich
EA	Elemental analysis
EDX	Energy dispersive X-ray
FAO	Food and Agriculture Organization
FTIR	Fourier transform Infra-red
HMS	Hexagonal mesoporous silica
K-C	Koble-Corrigan
MB	Methylene blue
MDR	Modified Dose-Response model
MPSD	Marquardt's percent standard deviation
OMC	Ordered mesoporous carbon
RB	Riboflavin
R-P	Redlich-Peterson
TEM	Transmission electron microscopy
TGA	Thermogravimetric analysis
WHO	World Health Organization
XRD	X-ray diffraction

KARBON MESOLIANG TERSUSUN DAN PENJERAP ALGINAT
KOMPOSIT: SINTESIS, PENCIRIAN DAN PRESTASI PENJERAPAN
UNTUK METILENA BIRU, KLORAMFENIKOL DAN RIBOFLAVIN

ABSTRAK

Karbon mesoliang tersusun (KMT) telah disintesis menerusi kaedah tempa nano menggunakan silika mesoliang heksagonal (SMH) sebagai templat dan polietilena glikol 400 (PEG-400) sebagai sumber karbon. Pendekatan eksperimen pemboleh ubah satu-masa telah digunakan untuk mengkaji kesan parameter proses terpilih termasuk suhu pengkarbonan (873-1073 K), masa penahanan (15-240 min), kadar pemanasan (1-10 K.min⁻¹) dan muatan PEG-400 (2.5-15 g) ke atas sifat-sifat luas permukaan, hasil dan kebolehan untuk menyingkirkan metilena biru (MB). Sampel ABA-16 telah memaparkan luas permukaan tertinggi 1026 m².g⁻¹ dengan jumlah isipadu liang 0.9976 cm³.g⁻¹ dan purata diameter liang 3.89 nm. Kehadiran struktur heksagonal tersusun dalam SMH dan KMT telah dilihat menerusi mikroskopi transmisi elektron (MTE). Persembahan penjerapan ABA-16 dan MABA-16 ke atas pewarna MB, antibiotik kloramfenikol (CPC) dan vitamin riboflavin (RB) diselidik menerusi operasi berkelompok dan turus. Penjerapan berkelompok telah dijalankan ke atas kepekatan awal 50-500 mg.L⁻¹ (MB) dan 50-400 mg.L⁻¹ (CPC dan RB), suhu (303-323 K) dan pH 3-11 untuk MB dan CPC manakala pH 3-7 untuk RB. Kapasiti penjerapan mono lapisan, Q_m tertinggi ialah 395 dan 620 mg.g⁻¹ (MB), 210 dan 223 mg.g⁻¹ (CPC) manakala 464 dan 222 mg.g⁻¹ (RB) oleh penjerap ABA-16 dan MABA-16. Pada semua keadaan, model lengkung garis sesuhu penjerapan tiga parameter menghasilkan padanan yang lebih baik

berbanding model lengkuk garis sesuhu dua parameter. Turut ditemui ialah model kinetik pseudo tertib kedua yang mempunyai padanan data eksperimen yang lebih baik berbanding model lain untuk penjerapan MB dan CPC. Manakala data eksperimen RB dipuaskan oleh model Elovich pada kepekatan awal yang rendah dan model kinetik pseudo tertib kedua pada kepekatan awal yang tinggi. Kajian termodinamik mencadangkan penjerapan MB, CPC and RB oleh ABA-16 dan MABA-16 tidak menggalakkan seiring dengan peningkatan suhu. Manik komposit alginat-karbon disediakan daripada ABA-16 dan MABA-16 telah digunakan untuk operasi turus di bawah keadaan berikut; kadar aliran ($10-30 \text{ mL.min}^{-1}$), kepekatan awal ($50-200 \text{ mg.L}^{-1}$) dan tinggi lapisan (2-6 cm). Model dos-respon terubahsuai (MDR) adalah paling baik untuk menerangkan perwatakan dinamik penjerapan turus. Kemosrotan ambilan sebanyak 27.7, 4.0 dan 15.8 % telah disaksikan ke atas manik komposit yang digunakan berdasarkan pendedahan terhadap lima kitaran proses penjerapan/penyahjerapan. Sebagai kesimpulan, PEG-400 yang tidak boleh dimakan terbukti berdaya saing sebagai sumber karbon untuk KMT berikutan sifat-sifat keselamatan, kos rendah dan juga mesra alam. Penjerap-penjerap yang dihasilkan telah menunjukkan prestasi penjerapan yang cemerlang untuk kedua-dua operasi penjerapan berkelompok dan turus.

**ORDERED MESOPOROUS CARBONS AND ITS ALGINATE COMPOSITE
ADSORBENTS: SYNTHESSES, CHARACTERIZATIONS AND
ADSORPTION PERFORMANCES FOR METHYLENE BLUE,
CHLORAMPHENICOL AND RIBOFLAVIN**

ABSTRACT

Ordered mesoporous carbons (OMC) were synthesized through nanocasting method by using lab-synthesized hexagonal mesoporous silica (HMS) as a template and polyethylene glycol 400 (PEG-400) as a carbon source. One-time variable experimental approach was deployed to study the effect of selected process parameters including carbonization temperature (873-1073 K), dwelling time (15-240 min), heating rate (1-10 K.min⁻¹) and PEG-400 (2.5-15 g) loading on the surface area properties, yields and its ability to remove methylene blue (MB). ABA-16 sample has displayed the highest surface area of 1026 m².g⁻¹ with the total pore volume of 0.9976 cm³.g⁻¹ and the average pore diameter of 3.89 nm. The presence of ordered hexagonal structure in HMS and OMCs was visualized through transmission electron microscopy (TEM). Adsorption performances of ABA-16 and MABA-16 on MB dye, chloramphenicol (CPC) antibiotic and riboflavin (RB) vitamin were investigated through batch and column operations. Batch adsorption studies was conducted at initial concentrations ranging from 50-500 mg.L⁻¹ (MB) and 50-400 mg.L⁻¹ (CPC and RB), temperatures (303-323 K) and pH ranging from 3-11 for MB and CPC while pH 3-7 for RB, respectively. The highest monolayer adsorption capacity, Q_m was 395 and 620 mg.g⁻¹ (MB), 210 and 223 mg.g⁻¹ (CPC) and 464 and 222 mg.g⁻¹ (RB) in respect to ABA-16 and MABA-16 adsorbents. At all conditions,

three-parameter adsorption isotherm models produced better fittings than the two-parameter models. It was found that pseudo-second order kinetic model fitted the experimental data better than other models for MB and CPC adsorption. As for RB, the experimental data was satisfied by Elovich model at lower concentration range while pseudo-second order kinetic model could be used to describe the upper concentration range. Thermodynamics studies suggested that MB, CPC and RB adsorption on ABA-16 and MABA-16 were not in favour to increasing temperature. Alginate-carbon composite beads prepared from ABA-16 and MABA-16 were used for column operation under the following conditions; flow rates ($10-30 \text{ mL}\cdot\text{min}^{-1}$), initial concentrations ($50-200 \text{ mg}\cdot\text{L}^{-1}$) and bed heights (2-6 cm). Modified dose-response (MDR) model was the best model to describe dynamic behaviour of column adsorption. The decrease of 27.7, 4.0 and 15.8 % uptakes were observed on the respective composite beads upon exposure to five cycle adsorption/desorption process. As conclusions, the non-edible PEG-400 has been proven to be a viable carbon precursor for OMCs due to its safety and environmental benign properties. The produced adsorbents have displayed excellent adsorption performances for both batch and column adsorption operations.

CHAPTER ONE

INTRODUCTION

1.1 Ordered mesoporous carbons

Credible contributions and performances of porous materials in the area of chemical manufacturing and processes, medicines and healthcare, electronic devices and environmental has long been acknowledged through employments of materials based on carbons, bio-sorbents, inorganic metals, clays, alumina and silica (Bhatnagar et al., 2011, Sen Gupta and Bhattacharyya, 2011). Higher activities and performances of such materials are mainly attributed to the presence of countless pores and consequently increase the total surface area. However, some limitations are inevitable such as mass transfer resistance, restricted selectivity and preference on target species etc. particularly due to dissimilarity in pore size and shape, and its distribution on the surface of the materials.

To break the limits, a new type of ordered porous materials with homogenous array of pores and channels networks of the similar size and shape has been proposed. Since then, the idea has become a testing ground for many scientists to manifest their knowledge and know how in formulating the best possible synthesis routes. Advancement in nanotechnology has enabled human to test their limits in tailoring and customizing the produced materials at atomic scale. The test has proven to be a big success for a group of researchers in Mobile Laboratories Company through innovation of cubic type ordered mesoporous silica, MCM-n family (Kresge et al., 1992). Soon after, researchers from University of California, Santa Barbara have declared a novel innovation of SBA-15, a hexagonal type ordered mesoporous silica (Zhao et al., 1998). These findings have been regarded as a major breakthrough

in conceptualizing the true synthesis of nano scale ordered structure materials as both of the silica families can be adapted as templates for other functional materials. By using a 'moulding' technique at nano scale on thermally stable MCM-48 ordered mesoporous silica, an original discovery of ordered mesoporous carbon has been reported by a group of Korean researchers (Ryoo et al., 1999).

Ordered mesoporous carbon is a new generation of carbonaceous molecular sieve synthesized through soft or hard template synthesis (Nishihara and Kyotani, 2012, Huang et al., 2012). Hard-templating or nanocasting is the most widely applied method where the carbon sources inversely replicating the ordered mesoporous structured of its template. An example of successful nanocasting process is shown through TEM images of the SBA-15 and KIT-6 (templates) and its carbon replica CMK-3 and CMK-8 in Plate 1.1.

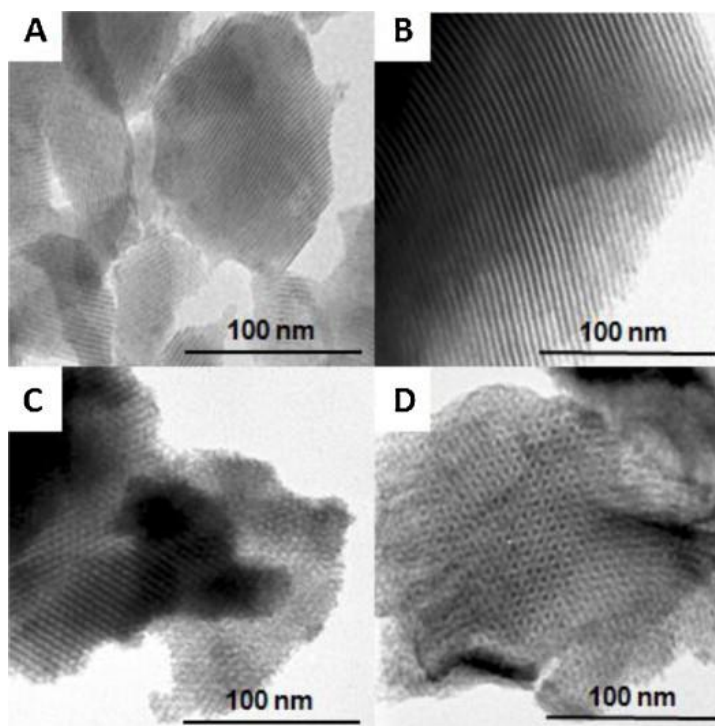


Plate 1.1 TEM images of (A) SBA-15 (template) (B) CMK-3 (carbon replica), (C) KIT-6 (template) and (D) CMK-8 (carbon replica). (Goscianska et al., 2013)

According to the reputable ISI-indexed scientific articles digital library database, the latest search using "ordered mesoporous carbon" key word has resulted in total of only 621 articles up to August 2014 (Scopus, 2014). The first term of ordered mesoporous carbon was detected in year 2002 with a total of publication of 1 article. Figure 1.1 shows the progress in publications related to ordered mesoporous carbon from 2002 to 2014. Initially, the progress in this research area is very slow with less than 15 articles have been published in the first five years. Progressively, researchers have realized the future potential of this magnificent material in many industrial applications. Starting from 2009, the number of publications has jumped swiftly from 52 articles per year up to almost 124 articles in the latest 2013 data. For comparison, more than 21000 publications related to "activated carbon" have been recorded within 1974 to 2014 time period. The difference shows that the specific research dedicated to ordered mesoporous carbon is still insufficient and small.

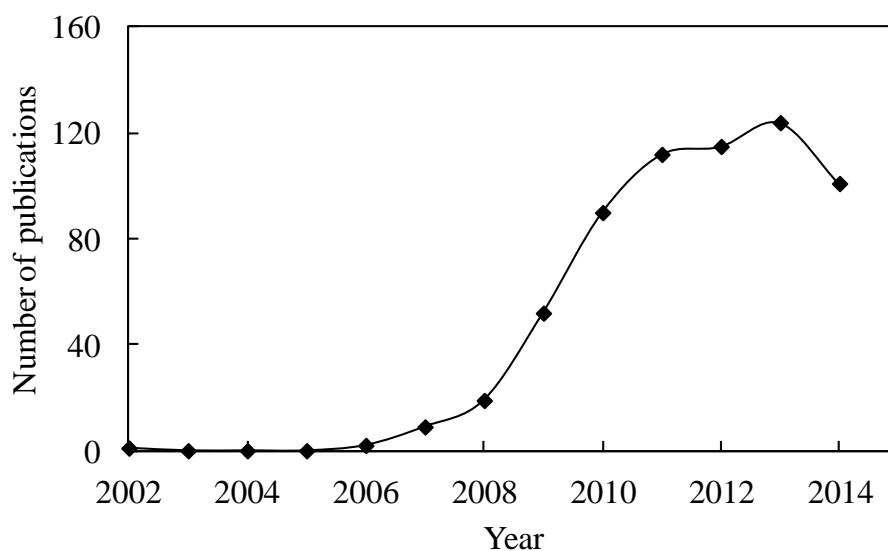


Figure 1.1 The progress in articles publications (ISI-cited) related to ordered mesoporous carbon (key word: ordered mesoporous carbon, date of search: 22/08/2014)

Complicated and complex material synthesis procedures, shortage in research funds and monetary assistances as well as lacking of advanced material inspection tools to support material characterization works might be the reason for such occurrence. The biggest numbers of articles were originated from China, South Korea, USA and Japan.

1.2 Alginate composite adsorbents

Recently, many studies have been dedicated for the preparation of low cost biosorbent composite derived from natural polymers such as chitin, chitosan, cyclodextrin and alginate (Tsiptsias et al., 2009, Keramati and Ghoreysi, 2014, Hu et al., 2011, Hassan et al., 2014). These polysaccharides possess good physiochemical characteristics, chemical stability, high reactivity and excellent selectivity towards various contaminants. In addition, polysaccharides are abundantly available, non-depleted and biodegradable. These features have made the materials attractive to be combined with other functional materials. Alginate is water-soluble linear polysaccharide extracted from brown seaweed and comprising of alternating blocks of 1-4 linked α -L-guluronic and β -D-mannuronic acid fragments that can be cross-linked with divalent ions to form sphere shape beads (Niñã et al., 2007). Fine particle size and costly material have restricted the use of ordered mesoporous carbons for column operation. Alginate-activated carbon composite has proven to be a very good sorptive material for dyes, organic compounds and metals (Hassan et al., 2014, Park et al., 2007, Lin et al., 2005). Enhancement of the adsorption is mainly attributed to the synergistic effect arising from marrying these two materials. Since alginate has a very good compatibility with carbon material, a combination of

ordered mesoporous carbon with alginate is rather promising for water treatment and product recovery solutions.

1.3 Dyes and pharmaceutical compounds

Recovery of dyes and pharmaceutical compounds from aqueous phase is increasingly important from the environmental and manufacturing perspectives. Nowadays, environmental concerns on water pollution related to improper effluent treatment and unlawful discharge has become a global issue. Around the world, many types of pollutants have entered fresh water streams, directly and indirectly to cause the affected water unsafe for consumption by human and animals, killing the water vegetation and downgrading the aesthetical surrounding appearance via bad odours and colour changes. Presence of dyes in water at 1 mg/L concentration level is enough to cause a noticeable colour change on the affected stream. Dyes are categorized as one of the main water pollutants due to mass discharge of the effluents from water intensified textile dyeing processes, food and beverages manufacturing, cosmetics, paint and coatings, printing and plastic based industries. It is estimated that the global demand for the dyes and organic pigments increases 3.9% annually up to USD 16.2 billion in 2013 (Freedonia, 2009). It is equivalent to 3.5% increment up to 2.3 million metric tonnes of dyes by volume.

Usage of antibiotics in livestock, poultry and aqua farming has been banned in most part of the world due to its adverse effect towards human health. However, illegal usage continues in the South Asian region including Vietnam, Malaysia and China; mainly under pressure to keep the farming operation profitable at the lowest cost possible. From 2009 - 2013, six Malaysia exporters have been included in the Import Alert 16-124 due to detection of chloramphenicol in their exported shrimp

products to USA (FDA, 2013). Chloramphenicol is one of the common antibiotics used as feed additives and growth promoters. In aqua farming, the feedstock is distributed straight into the water thus simultaneously releasing the antibiotics in the water stream. There is a growing concern on the formation of new strains of germs that immune to the antibiotics. Prolong accidental exposure even at tiny dose also can possibly cause human to be resistance towards the antibiotics; thus, making the existing or future diseases difficult or impossible to be cured. According to Food Regulations 1985, chloramphenicol is listed as prohibited drugs for food along with nitrofurans and Beta agonists excluding Ractopamine (Laws of Malaysia, 2011). The presence of pharmaceuticals and related drugs in open local environment has been detected in Langkat River Basin, Selangor (refer to Figure 1.2) based on the recent environmental monitoring study (Al-Odaini et al., 2013). Therefore, considerable efforts to setup an effective and systematic pharmaceuticals and clinical waste disposal system are commendable.

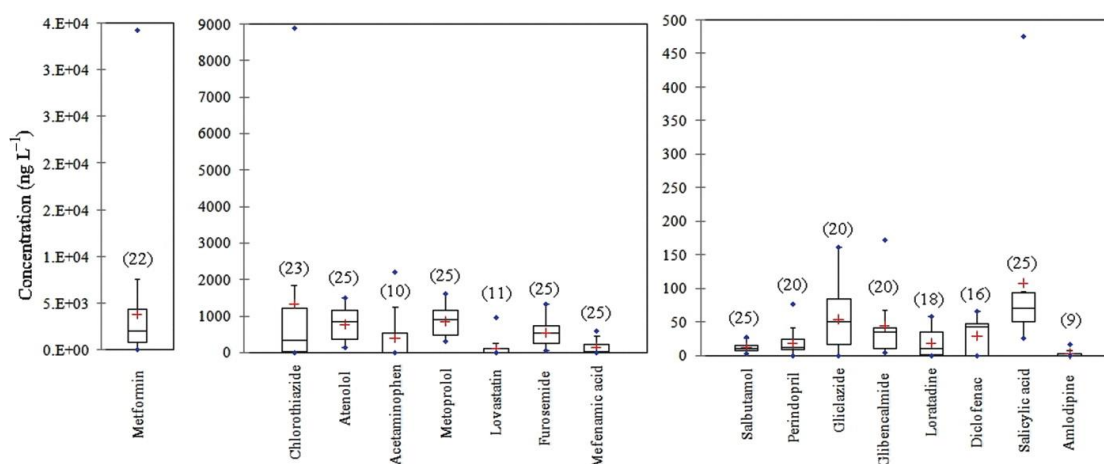


Figure 1.2 Pharmaceutical waste detected in sewage treatment plant near Langkat River, Selangor (Al-Odaini et al., 2013)

Unlike antibiotics, an adverse effect of vitamins on environment is rarely discussed. However, these substances are known to cause positive alteration of biological activities in living cells. Vitamins are mostly acquired from daily food intakes such as milk, vegetables and meats. Unfortunately, vitamin deficiencies are common to most people in Central Africa and Southern Asia due to poverty and political unrest which causing them poor access to nutritious food. It is estimated that two billions people around the globe mostly children and reproductive mothers are affected with vitamins (A, riboflavin, thiamine, niacin, folate and C) and minerals (iron and calcium) deficiencies. To combat this issue, selected food such as dried skimmed milk, vegetable oil and wheat flour are fortified according to recommended WHO and FAO guidelines (WHO and FAO, 2006). Supplementation programme through distribution of multivitamin and mineral pills was found to be very helpful to increase the level of uptakes. Riboflavin is listed as a permitted food colorant in many countries including European Union countries, Japan and Malaysia (Feingold, 2012).

Pharmaceutical companies have scaling up their production capacity to meet up with the global demands. Major progresses in the area of biotechnology have contributed to bigger and cheaper production cost. It is now estimated that 90% of the riboflavin production is made via biotechnology fermentation route instead of chemical synthesis using highly toxic chemicals, among other includes aniline (BIO, 2013). Riboflavin or known as vitamin B2 is one of the components for vitamin B complex built up is essential for energy metabolism, red blood cell production and nerve system maintenance. Riboflavin is soluble in water therefore; a study on its adsorption characteristics from aqueous phase is valuable for the future product recovery and purification purpose.

1.4 Adsorption process

Adsorption process is one of the prevalence methods employed in separation and purification area particularly for removal of pollutants from waste water and industrial product recovery. Adsorption is defined as an accumulation of solutes on the solid adsorbent surface as a results from either electrostatic forces or/and chemical interactions between the solutes and the adsorbents. A vast number of references reporting on the adsorption of dyes, heavy metals, organic contaminants and bio-molecules are available from printed or electronic database. The most common reported adsorbents include activated carbons, dried plant materials, clays, and silica. These materials are suitable adsorbents owing to its high surface area and porosity properties, high distribution of active functional groups on the surfaces and mostly inert for the selected applications.

Recently, a few advanced materials have been successfully adapted as adsorbents including siliceous and carbon based ordered mesoporous materials. These materials display excellent adsorption performance towards bulky molecules such as complex dyes and bio-molecules owing to its intrinsic ordered structure, higher surface area and pore volume with narrow mesopore size distribution. The uniform shape and array of pores and channels networks provide lower mass transfer resistance to selective solutes thus enhancing the overall adsorption capacities.

1.5 Problem statement

Selecting an appropriate organic carbon precursor for nanocasting of ordered mesoporous carbons is essential for economical and environmental reasons. Currently, ordered mesoporous carbons are mainly derived from edible or hazardous organics. Organics edible sources like monosaccharides (glucose and fructose) and

disaccharides (sucrose) were frequently reported in the literature (Cai et al., 2014, Kubo et al., 2011, Joo et al., 2001, Yu et al., 2001, Kruk et al., 2000). The substances were predominantly selected due to high carbon content and easiness to hydrolyze in water. However, the usage of the edible sources for non-edible purposes might possibly cause a subtle issue associating to global food security. Sugars are one of the vital ingredients in our food for supplying instant energy to the body and improving the taste of the food. The usage of sugars in commercial non-edible sectors might drive up the global sugar price and cause short supply around the world. As a response, a few successful attempts have been made by using non-edible carbon sources in the nanocasting process. Unfortunately, some of them are highly toxic, environmentally hostile and require stringent handling and disposal procedures (Tian et al., 2011, Lázaro et al., 2007). In this research, a bulk chemical of polyethylene glycol 400 has been proposed as an alternative carbon precursor. Polyethylene glycol 400 is relatively cheaper, abundantly available for commercial use and softer to environment too.

Secondly, the biocompatibility advantage of porous carbon is generally recognized. Adsorption and separation of pharmaceutical compounds and biomolecules such as vitamins, drugs, antibiotics and proteins are important due to expanding applications in drug delivery, biosensors and medical device coatings (Liu et al., 2013, Walcarius, 2012, Basiaga et al., 2011). The unethical disposals of drugs and antibiotics by consumers and industry players have post another danger to environment and life forms. These contaminants, including their precursor compounds and transformation products, are discharged into the environment intentionally and unintentionally during manufacturing processes and through consumption or disposal of used and unwanted drugs (Daughton and Ternes, 1999).

In addition, chemical routes to produce vitamins are proven to be more expensive and harmful to environment because of the use of toxic substances. Alternatively, bio-fermentation method using various fungi, yeast and microbes offers relatively cheaper operational cost and environmental friendly solution; however, the route requires efficient purification and separation process for product recovery purpose. Insufficient mesoporosity and complicated pores and channels networks in conventional carbon adsorbents have limited its performance against bulky bio-molecules. Hence, ordered mesoporous carbon is proposed to obtain optimum degree of separation and removal of the targeted bulky molecules used in this research.

On another perspective, the physical appearance of the adsorbent plays a major role for effective adsorption process. The usage of unsuitable particle size in adsorption column, for example; can cause high pressure drop and blockage. Usually, the problem is solved by substituting the fine particles with granular, pellet, spherical or bead adsorbents. Reshaping and resizing of powder/fine particles can be done through mechanical and chemical processes such as extrusion, granulation and encapsulation with bio-polymeric materials (Ouyang et al., 2013, Auta and Hameed, 2013, Rizhikovs et al., 2012). Encapsulation of carbon by chitosan, starch, cyclodextrin and recently, alginate is commercially viable for production of low-cost adsorbent because they are cheaper, available in bulk quantities, naturally non-toxic and flexible to be combined with other functional materials (Kumar et al., 2013, Crini, 2005).

Enhancement in adsorption performance could be realized by performing appropriate modification on the physical or chemical properties of the adsorbents. Surface chemistry of carbon adsorbents could be easily modified by using various chemicals and means without compromising its porosity and large surface area

properties. Post modification routes frequently involved chemical impregnation including wet oxidation method, metal doping and chemical vapor deposition (Moradi, 2014, Cheah et al., 2013, Florent et al., 2013, Ran et al., 2013, Moradi et al., 2010). Impregnation with acid and base solutions is preferred due to its simplicity and straight forward procedure. Acetic acid is used in this work to enhance the intensity of oxygenated active groups on the carbon surface and subsequently the performance of non-modified and modified ordered mesoporous carbons are evaluated for its adsorption performance on targeted adsorbates.

1.6 Research objectives

This research is fulfilling the following objectives to:

- (a) synthesis ordered mesoporous carbons from non-edible carbon source, polyethylene glycol 400 through nanocasting method using self-synthesized hexagonal mesoporous silica as a template.
- (b) perform comprehensive physical and chemical characteristics analyses on the synthesized ordered mesoporous materials by using various analytical and inspection tools.
- (c) investigate the adsorption of selected solutes; methylene blue (dye), chloramphenicol (antibiotic) and riboflavin (vitamin) on the synthesized non-modified and modified ordered mesoporous carbons under varying operational parameters such as initial concentrations, temperatures and pH of solutions.
- (d) evaluate the isotherms, kinetics and thermodynamics of the selected solutes adsorption on the synthesized non-modified and modified ordered mesoporous carbon adsorbents.

- (e) determine the breakthrough dynamics and characteristics of the selected solutes on the synthesized non-modified and modified ordered mesoporous carbon-alginate composite adsorbents under varying operational parameters; flow rate, initial concentration and bed height.
- (f) evaluate the reusability of the selected non-modified and modified ordered mesoporous carbon-alginate composite adsorbents through five cycle in-situ column regeneration studies.

1.7 Scope of research

The study is deliberately conducted be either in stages or in parallel mode connecting three research components comprising the syntheses of materials, materials characterizations and adsorption works. Each of work is carefully planned and executed to satisfy the outlined research objectives.

Syntheses of materials involve the preparation of hexagonal mesoporous silica that subsequently to be adapted as a template for nanocasting of ordered mesoporous carbons from polyethylene glycol 400. Effects of carbonization temperature, dwelling time, heating rates and PEG-400 loading on the yields of carbons and methylene blue removal performance are investigated thoroughly. Extensive material characterizations involving transmission electron microscopy and X-ray diffraction analysis are obligatory at this stage to inspect the presence of ordered structure within the materials. The quality wise of the produced ordered mesoporous carbons are also inspected for their porosity and surface area properties.

A series of batch adsorption experiments are conducted to investigate the produced ordered mesoporous carbons adsorptive properties against water-soluble

complex bulky molecules. A methylene blue dye, a chloramphenicol antibiotic and a riboflavin vitamin are selected as model adsorbates. A fraction of ordered mesoporous carbons are subjected to modification with acetic acid to enhance the presence of oxygenated active groups on the carbon surface. The surface chemistry and adsorption performance are investigated for comparison study. The collected adsorption data are tested on various two and three parameters adsorption isotherm model and kinetic models to understand the possible mechanisms involved in the sorption process, including the thermodynamic properties.

For column operation, new ordered mesoporous carbon-alginate composite beads are prepared by cross-linking the carbon-alginate mixture in calcium chloride solutions. The freeze dried composite beads are packed in the column and tested for the methylene blue, chloramphenicol and riboflavin removal. The experimental data are fitted to Thomas, modified dose-response (MDR) and bed-depth service time (BDST) models. In-situ semi batch regeneration studies using ethanol as solvent are conducted for five cycles to determine the adsorbent reusability.

Auxiliary material characterizations inclusive of scanning electron microscopy, electron diffraction microscopy, elemental analysis, proximate analysis, determination of pH_{zpc} are also investigated to provide additional information that can be correlated to the overall adsorption performances.

1.8 Organization of the thesis

The thesis is divided into five main chapters. Each chapter is academically written to present the true and original findings related to the respective research topic.

Chapter one is designed to provide a brief introduction of the overall research works based on the selected key words. Problem statements are brought to the attention explaining the rationale and significance of the research. The presented objectives are pointed one-by-one in a clear and progressive order.

Chapter two presents the comprehensive review on the related research backgrounds. The first part of the chapter elaborates in details the ordered mesoporous carbons progress in modern history, synthesis method and applications particularly in liquid phase adsorption. In a meanwhile, the second part summarizes the know-how of the advancement in adsorption technology and science and its theoretical knowledge for the batch and continuous adsorption operation.

The details of the materials and methods applied in this research are elaborated in Chapter three. The chapter is divided into three parts to represent material syntheses, adsorption and adsorbent regeneration studies, material characterizations and last but not least environmental sustainability and safety culture precautions in support to safer and greener research conduct.

Chapter four is divided into three sections. The first section is mainly discussed the findings on the material synthesis and characterizations. The second section presents the results and discussion of the batch adsorption system covering the aspects of adsorption equilibriums, two and three-parameter isotherm models, kinetics and thermodynamics. The results for continuous adsorption are given out in section three. The final section is reserved mainly for continuous regeneration studies on the selected adsorbents.

The last chapter five presents the research conclusions and future recommendations.

CHAPTER TWO

LITERATURE REVIEW

Chapter two briefly presents the past findings and reviews available from credible scientific database and references that related to this research topic. In general, the chapter outlined the backgrounds and development of ordered mesoporous materials area particularly ordered mesoporous carbons that include the synthesis methods and the material properties. Then, a review on the use of alginate carbon composite is presented to signify their use in this research. Next, an extensive review of the adsorption process is presented covering the selected adsorption process variables, isotherms, thermodynamics, kinetics and dynamic adsorption models, to list a few.

2.0 Ordered mesoporous materials

“If nanotechnology, the manipulation of matter at the atomic level, at maturity achieves even a fraction of its promise, it will force the reassessment of global markets and economies and industries on a scale never experienced before in human history.”

J. Canton

Institute of Global Future, Sept. 2000

Echoing the abovementioned statement, it is so true that an inception of porous materials in unlimited modern applications has caused inexorable progresses to the modernization of the world. Since the first commercialization of activated carbon 200 years ago, human have employed a wide range of porous materials be either harvesting it's from resourceful nature or through man-made chemical

syntheses. Today's we are entering a new frontier of advanced material science where material scientist and engineers are now destined to have a right and ability in controlling the shape, arrangement and size of pores structures at nano scale level (Joo et al., 2001, Kruk et al., 2000, Ryoo et al., 1999, Kresge et al., 1992). Such detailed features only can be achieved through appropriate synthesis techniques that integrate human achievement in understanding delicate material chemistry science and nanotechnology.

Ordered mesoporous materials are featured by identical pores in similar size and shape distributed in orderly manner within the materials; unlike the conventional porous materials that garnered the porosity from both micro- and mesopores with heterogeneous pore size and shape. Ordered mesoporous silica, ordered mesoporous metal oxides and ordered mesoporous carbons are common example of ordered mesoporous materials (Zhu et al., 2014, Jin et al., 2012, AlOthman and Aplett, 2010, Jo et al., 2009, Hyodo et al., 2003). Handful literatures related to the syntheses and applications of ordered mesoporous materials are available for referencing purposes (Xia et al., 2010, Lu and Schüth, 2005).

For a long time carbon materials has been regarded as a material with countless applications. Carbon based materials like ordered mesoporous carbons are scientifically attractive due to their inert nature to most of the compounds, rigid structural integrity that suits many industrial applications and exceptional mesoporosity and chemistry properties; in which, contributing to a good adsorptive potential. In addition, ordered mesoporous carbons can be easily functionalized to enhance its performance towards specific targeted chemical species and applications (Moradi, 2014, Florent et al., 2013, Lázaro et al., 2007).

2.1 Ordered mesoporous carbons

A humble beginning in producing porous carbon for bronze manufacturing has dated back thousands years ago by the Egyptians and Sumerians. As for the modern record, Bussy is the first man to incorporate the thermal and chemical processes for activated carbon production (Hassler, 1974). In the early of 20th century, Van Ostrejko commercialized the production of activated carbon by impregnating metallic chlorides to carbonaceous material before carbonization and introduced mild oxidation of charred material to carbon dioxide or steam at high temperature (Smâiések and éCernây, 1970). Since then, a numerous studies have been devoted to enhance activated carbon quality in terms of porosity, surface area, pore size distribution, functionality and selectivity, to list a few (Mohamad Nor et al., 2013, Hoseinzadeh Hesas et al., 2013, Dias et al., 2007).

A recent finding reported a preparation of activated carbon from date stone by H₃PO₄ impregnation and followed by activation at high temperature has produced the maximum total surface area of 1225 m².g⁻¹ (Danish et al., 2014). Plate 2.1 shows wide-range of pore sizes and shapes that unevenly distributed on the surface of the material; a typical feature for activated carbon prepared from biomass. It is evidence that the produced carbon material is porous but having a low degree of structural ordering. Similar findings can be found here (ElShafei et al., 2014, Hassan et al., 2014, Gundogdu et al., 2013, Cherifi et al., 2013).

In year of 1999, a group of Korean researchers has shocked the nanoscience experts by announcing the novel synthesis of world's first ordered mesoporous carbons derived from sucrose by using ordered mesoporous silica, MCM-48 as a template (Ryoo et al., 1999).

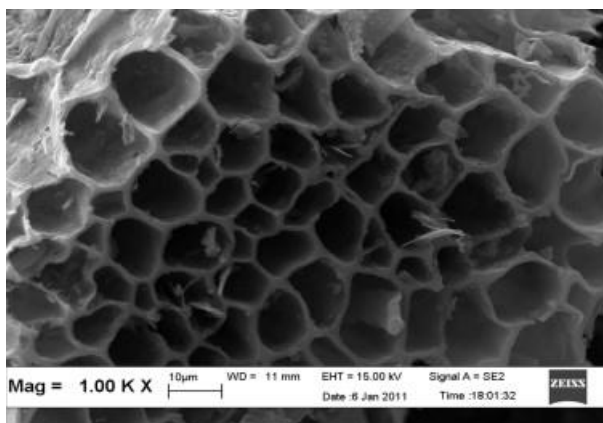


Plate 2.1 SEM image of activated carbon produced from banana frond (Foo et al., 2013)

The discovery has stamped a new chapter in porous material synthesis fields by setting up a new breakthrough for human to produce highly ordered porous carbons. More or less, they are very much owing to the invention of ordered mesoporous silica reported 7-8 years before; in which, has enabled them to use MCM silica family as a template for their carbon replica (Kresge et al., 1992). Guo et al., (2013) defined ordered mesoporous carbons as materials that possessed regular and tuneable pore size, as well as stable frameworks with pore surfaces easy for modification or functionalization (Guo et al., 2013). An example of ordered hollow channels in ordered mesoporous carbons is illustrated in Plate 2.2 (Cai et al., 2013).

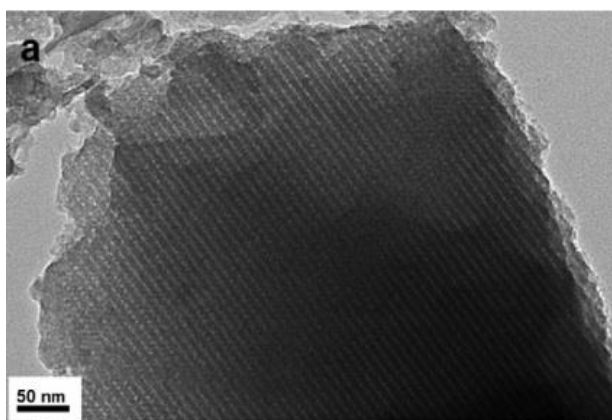


Plate 2.2 TEM of ordered mesoporous carbon derived from phenol/formaldehyde as a carbon source (Cai et al., 2013)

Like other carbon materials, ordered mesoporous carbons are known to have unlimited potential for wide range of applications in environment, medical, pharmaceuticals, gas and energy storage, catalyst, electrochemical and etc. (Tripathi et al., 2014, Zhu et al., 2014, Yu et al., 2013, Walcarius, 2012, Tüysüz and Schüth, 2012, Zhao et al., 2012, Kockrick et al., 2010). A previous work on the adsorption of various dyes on ordered mesoporous carbon concluded that fast adsorption rate of CMK-5 is due to its tubular mesostructures, bimodal mesopore system and high surface area properties (Hao et al., 2010). They reported the maximum adsorption capacity of 733, 1131 and 1403 mg.g⁻¹ for reactive blue 19, acid red 57 and fuchsin basic, respectively. High adsorption capacities observed in the recent adsorption studies of alkaloids proved that OMCs have an excellent biocompatibility towards pharmaceutical compounds. Berberine hydrochloride, colchicine and matrine have shown the maximum adsorption capacities up to 450, 600 and 680 mg.g⁻¹, respectively (Li et al., 2013b).

Unlike its predecessors i.e. conventional mesoporous carbons and activated carbons, OMCs have extra advantages such as periodic pore symmetry, large pore volume, high specific surface area, centralized mesopore distribution, and tuneable pore diameter (Yuan et al., 2007). These features have made OMCs as better material to be exploited as carbon molecular sieves for the adsorption of bulky molecules from liquid solutions such as dyes and bio-molecules.

2.2 Synthesis of ordered mesoporous carbons

Synthesis of OMCs involved a delicate chemistry and physical processes. Ordered mesoporous carbons can be synthesized through template carbonization routes. According to Kyotani, template carbonization involved the carbonization of

an organic compound in the nano space of a template inorganic substance and the recovery of the resultant carbon from the template. Template carbonization allows the preparation of carbon materials with controlled architecture and relatively narrow pore size distribution (Fuertes, 2003). The basic concept of this method is to produce carbon replica that can imitate the pores properties of its template (Kyotani, 2000, Bandosz et al., 1994). In one of the earliest works significant to template carbonization, Kyotani and Tomita have synthesized ultra-thin graphite film from the carbonization of organic polymer in the two-dimensional opening between the lamellae of layered clay such as montmorillonite (Kyotani et al., 1988).

The template carbonization routes can be classified as hard-templating or soft-templating; based on the types of templates used during carbonization. The 'hard-templating' term is gradually evolved to a new term; nanocasting, in describing its challenging and wider applications at nano scale level (Lu and Schüth, 2005, Han et al., 2003). A detailed review on the preparation of ordered mesoporous carbons techniques are presented in the following sections.

2.2.1 Nanocasting

Nanocasting is an extensive nano scale moulding method to produce an inverse replica of the parent template (Jones and Lodge, 2012, Huo, 2010). Generally, nanocasting of OMCs involves four stages in the following order (Xia et al., 2010):

- (i) The preparation of ordered mesoporous silica as a template.
- (ii) The infusion of a suitable carbon precursor into the template pores either by wet impregnation, chemical vapour deposition or a combination of both methods.

- (iii) The polymerisation and carbonisation of the carbon precursor to generate an organic–inorganic composite.
- (iv) The removal of the inorganic template to obtain a carbon replica.

Yu and co-researchers have illustrated a typical OMCs synthesis route from sugar by using silica sphere as a template as been depicted in Figure 2.1.

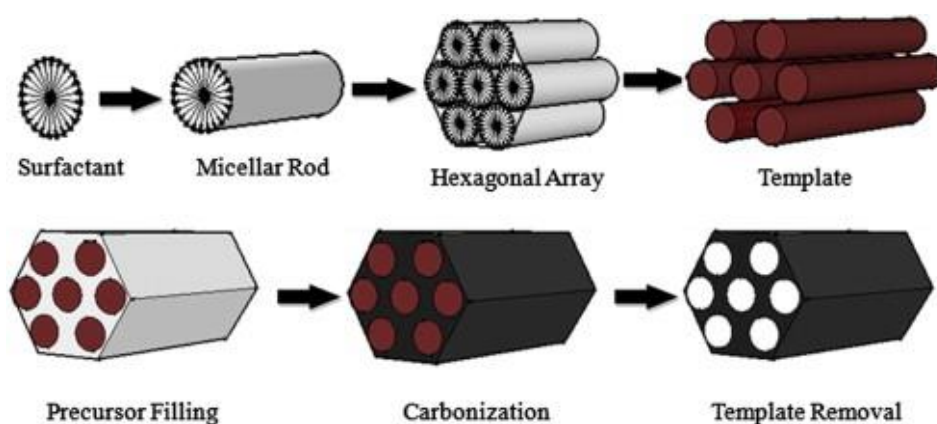


Figure 2.1 Synthesis route for highly ordered mesoporous carbon (Guo et al., 2013)

A proper selection of the template is critically important to ensure fruitful nanocasting process. The template should be able to maintain its structure integrity under excessive heat exposure, inert to carbon precursors and easily dissolved for recovery of pure carbon replica (Xia et al., 2010, Lu and Schüth, 2005). Ordered mesoporous silica seems a right template candidate that fulfilled the aforementioned criteria. MCM - Mobil Composition of Matter and SBA - Santa Barbara Amorphous ordered mesoporous silica families are the common templates employed for nanocasting of OMCs, and also included is KIT and FDU families (Goscianska et al., 2014, Enterría et al., 2014, Lin et al., 2012, Anbia and Salehi, 2012, Gokulakrishnan et al., 2011, Lu et al., 2005, Parmentier et al., 2003). The casting

process begins with the introduction of carbon precursor into the templates. To this date, sucrose is the most applied organic carbon precursor in nanocasting process (Goscianska et al., 2014, Lang et al., 2012, Smith and Lobo, 2006, Parmentier et al., 2004). In one of the recent studies, honey has been employed on SBA-15 template to produce OMCs (Lu et al., 2013).

At the beginning, edible carbon precursor like sucrose is attractive because it is naturally produced, cheap, can be easily hydrolyzed by acid and pose no hazard to environment. Unfortunately, a long haul deployment of edible sources to support mass production of OMCs is considered not sustainable while half of the world population is experiencing food shortage and increasing feedstock price. The future competition in using feedstock for non-edible purposes might stimulate higher demand for the commodity and subsequently drive the price increase; thus, limiting the poor people to have access to the feedstock. A similar issue has been highlighted in biofuel production concerning on the use of edible oils as energy fuel. Since then, a number of attempts have been reported on the use of non-edible oils for sustainable production of biofuel (Kumar and Sharma, 2011, Chhetri et al., 2008).

A selection of non-edible carbon precursors has been proposed and tested for OMCs nanocasting among others, furfuryl alcohol, glycerol, phenolic resin, divinylbenzene, petroleum pitch and propylene (Li et al., 2013a, Farzin Nejad et al., 2013, Lin et al., 2012, Ramasamy and Lee, 2010, Ignat et al., 2010, Kao and Hsu, 2008, Smith and Lobo, 2006, Yang and Sayari, 2005, Lu et al., 2004, Parmentier et al., 2004). However, some of the materials are toxic, hazardous, and flammable. In addition, the materials require stringent handling and storage to ensure safer working environment. PEG-400 is a viscous colourless liquid build by ethylene glycol monomer with the following properties i.e. non flammable, highly-soluble in water,

less hazardous to human and friendly to environment (Henning, 2001). PEG-400 is mainly used for adhesive, ink, lubricant, pharmaceutical, textile and wood industries (CARBOWAX, 2011). Optimal Chemicals (M) Sdn. Bhd., a joint venture local company between PETRONAS and Dow Chemical is currently producing polyethylene glycols at capacity of 15000 tonnes per year (OPTIMAL, 2014). Up to date, no official record is available on the attempt in using PEG-400 as carbon precursor for OMCs nanocasting.

Carbonization has a vital role in conversion of carbon precursor/template composite into a porous and rigid carbon replica. Carbonization is timely conducted at high temperature under inert atmosphere to obtain the optimum carbon conversion following the degradation of inorganic matter originated from the used carbon precursor. Immature carbonization could induce formation of poor quality carbon replica in deficient of structural integrity and purity. Table 2.1 summarizes some of the carbonization conditions employed for nanocasting of OMCs by the previous researchers.

The final step in nanocasting process is recovery of carbon replica from its template. Silica template can be removed by dissolving the material into sodium hydroxide (NaOH) or hydrofluoric acid (HF) solutions (Farzin Nejad et al., 2013, Tian et al., 2012, Kao and Hsu, 2008, Kim et al., 2005). Liu and co-workers performed the template removal with 1 M 1:1 (V/V) water-ethanol NaOH solution at temperature 373 K (Liu et al., 2006). Also, carbon/silica composite is immersed in 9.6 % HF solution at room temperature for 24 h to recover carbon replica (Ignat et al., 2010). Recently, many researchers opted to NaOH for safer alternative. Handling of NaOH is relatively easier than HF and does not require stringent safety precautions and apparatus.

Table 2.1 Various carbonization conditions applied for OMCs syntheses

Template	Precursor	Carbonization condition	Reference
SBA-15	Sucrose	T = 1173 K Vacuum	(Peng et al., 2014)
SBA-15	Sucrose	T = 1073 K t = 6 h Nitrogen	(Dong et al., 2012)
SBA-15	Furfuryl alcohol/TMB	T = 1123 K HR = 1-5 K/min t = 4 h Argon	(Tian et al., 2011)
SBA-15	Sucrose Glycerol	T = 1123 K t = 6 h Nitrogen	(Ignat and Popovici, 2011)
SBA-15	Glycerol	T = 1123 K HR = 1 K/min t = 5 h Nitrogen	(Ignat et al., 2010)
SBA-15	Furfuryl alcohol/TMB	T = 1123 K t = 4 h Nitrogen	(Hao et al., 2010)
SBA-15	Sucrose	T = 1173 K HR = 5 K/min Vacuum	(Liu et al., 2006)

T: temperature, HR: heating rate, t: dwelling time, TMB: trimethylbenzene